

A Highly Accurate Numerical Solution of a Biharmonic Equation

M. Arad¹, A. Yakhot¹, G. Ben-Dor¹

¹*Pearlstone Center for Aeronautical Engineering Studies
Department of Mechanical Engineering
Ben-Gurion University of the Negev
Beersheva 84105, Israel*

Received October 20, 1996; accepted February 3, 1997

The coefficients for a nine-point high-order accuracy discretization scheme for a biharmonic equation $\nabla^4 u = f(x, y)$ (∇^2 is the two-dimensional Laplacian operator) are derived. The biharmonic problem is defined on a rectangular domain with two types of boundary conditions: (1) u and $\partial^2 u / \partial n^2$ or (2) u and $\partial u / \partial n$ (where $\partial / \partial n$ is the normal to the boundary derivative) are specified at the boundary. For both considered cases, the truncation error for the suggested scheme is of the sixth-order $O(h^6)$ on a square mesh ($h_x = h_y = h$) and of the fourth-order $O(h_x^4, h_x^2 h_y^2, h_y^4)$ on an unequally spaced mesh. The biharmonic equation describes the deflection of loaded plates. The advantage of the suggested scheme is demonstrated for solving problems of the deflection of rectangular plates for cases of different boundary conditions: (1) a simply supported plate and (2) a plate with built-in edges. In order to demonstrate the high-order accuracy of the method, the numerical results are compared with exact solutions. © 1997 John Wiley & Sons, Inc. Numer Methods Partial Differential Eq **13**: 375–391, 1997

Keywords: Biharmonic equation; finite difference; high-order accuracy

I. INTRODUCTION

A computational solution of a partial differential equation (PDE) involves a discretization procedure by which the continuous equation is replaced by a discrete algebraic equation. The discretization procedure consists of an approximation of the derivatives in the governing PDE by differences of the dependent variables, which are computed only at discrete points (grid or mesh points). The discretization of the continuous problem inevitably introduces an error in computing the derivatives and, as a result, an error in the computational solution. In general, one starts with a given PDE and uses a discretization procedure for developing a finite-difference equation (FDE) that is a linear relation between discrete values of the unknown function computed on grid point. Then, with the aid of a Taylor series expansion about the node at which the derivative is evaluated, the PDE can be rewritten in the following form: PDE = FDE + TE, where the remainder, TE, is

the truncation error. The truncation error (TE) is the difference between the original PDE and its FDE approximation. It is expressed in terms of the Taylor series expansion and its lowest-order term gives the accuracy order of the discretization method applied to the original PDE. It should be noted that one can estimate the numerical solution error for a finite-difference representation as the order of the leading term in the remainder (TE), which can be considered as a close approximation to the error, provided that the grid size is small. However, the complete evaluation of the numerical solution error must be based on comparison with the exact solution.

One way of increasing the accuracy order of a discretization scheme is to set to zero as many as possible first terms of the TE. In 1941, Kantorovich and Krylov presented in a Russian edition of their book, the sixth-order accuracy nine-point discretization scheme for Poisson's equation. In 1964 the English edition of their book [1] appeared. After the *Mehrstellenverfahren* (*Hermitian* or *many-point*) procedure introduced by Collatz [2] in the early 1950s, different high-order finite-difference approximations for the Poisson and Helmholtz equations were developed. Young and Dauwalder [3] studied numerous such high-order nine-point schemes in great detail. For the general linear elliptic second-order partial differential equation, Young and Gregory [4] derived high-order discretization methods. They gave complete formulas and summarized the coefficients in a Table for the high-order nine-point discretization schemes of a quite general type. For example, the sixth-order accuracy scheme, developed in [1] for the Poisson equation can be derived as a particular case from the general Young and Gregory scheme [4].

Lynch and Rice [5] introduced a new high-order accuracy discretization procedure for the linear elliptic partial differential equations based on the High Order Differences with Identity Expansion (HODIE) method. Boisvert [6] used the HODIE method for solving elliptic boundary value problems on rectangles with Dirichlet boundary conditions. He derived the fourth- and sixth-order accuracy finite-difference discretization approximations of the Helmholtz equation. Similarly, the sixth-order approximation of the Helmholtz equation with Dirichlet boundary conditions on a rectangular domain was suggested by Houstis and Papatheodorou [7].

In the 1980s a considerable contribution in developing high-order-accurate finite-difference discretization schemes for elliptic partial differential equations was made by Manohar, Stephenson, and others [8–12]. The sixth-order 9-point discretization stencil for the Poisson equation with the Dirichlet boundary conditions on a rectangular domain was derived in [8]. For the Neumann boundary conditions, the authors presented the difference formulas with the second-order accuracy truncation error. They also described a possible procedure to obtain the fourth- and sixth-order schemes; however, the formulas were not given due to their claim that they become quite cumbersome. Monohar and Stephenson [9] introduced an efficient procedure for deriving the high-order (up to sixth) 9-point discretization scheme for the Helmholtz equation. They presented the difference formulas in an explicit form for the Dirichlet type boundary condition. The general case of the linear or quasi-linear elliptic equation of the second-order with variable coefficients was considered in [11]. A high-order finite-difference approximation was developed. The Taylor series expansion technique of the solution and the coefficients of the general elliptic equation was applied in [12] for developing high-order-accurate discretization schemes. The procedure is mathematically equivalent to that of Young and Dauwalder [3]. The Poisson or the Helmholtz equations are the particular cases of the difference schemes proposed in [11, 12].

In the present study we develop the high-order accuracy discretization scheme for a biharmonic equation $\nabla^4 u = f(x, y)$ (∇^2 is the two-dimensional Laplacian operator). To derive the high-order finite-difference scheme we used the symbolic operator procedure recently presented by us in [13]. According to this procedure, using the original PDE, the high-order derivatives of the Taylor series expansion of the TE are replaced by lower order derivatives, which require a smaller number of grid points in the discretization process. The standard difference schemes for the

biharmonic equation based on 13-point or 25-point stencils with the second- or the fourth-order accuracy, respectively, are well-known and can be found in [2]. The schemes require the use of fictitious points outside of the computational domain. Fourth-order 9-point stencil schemes without fictitious points were developed and tested in [14, 15]. We assume that the biharmonic equation is defined on a rectangular domain with two types of boundary conditions: (1) u and $\partial^2 u / \partial n^2$ or (2) u and $\partial u / \partial n$ (where $\partial / \partial n$ is the normal to the boundary derivative) are specified at the boundary. For both cases, we split a biharmonic equation into two Poisson equations. There is a considerable difference between the two considered cases. For the first case, the problem can be reduced to two Poisson equations with Dirichlet type boundary conditions when the high-order accuracy discretization schemes are well-known in the literature [1–12]. The second case is more complicated, because we obtain two coupled Poisson equations with mixed boundary conditions. The difficulty of this case is similar to that of the Neumann boundary condition for the Poisson equation. Kwon, Manohar, and Stephenson [14] considered this case and developed a fourth-order accuracy difference scheme. For this case, we derived a special algorithm for the discretization of the boundary conditions, which led to a high-order accuracy scheme. The truncation error for the suggested scheme is of the sixth-order $O(h^6)$ on a square mesh ($h_x = h_y = h$) and of the fourth-order $O(h_x^4, h_x^2 h_y^2, h_y^4)$ on an unequally spaced mesh. To the best of the authors' knowledge, the sixth-order nine-point numerical algorithm for approximating the biharmonic equation with mixed boundary conditions, developed in the course of this study, is not available in the open literature. Different numerical examples of the biharmonic problems from the theory of loaded plates are considered.

II. DEFINITIONS

Computational domain G . Let a rectangle $G = \{0 \leq x \leq l_x, 0 \leq y \leq l_y\}$ be a two-dimensional computational domain. Let two discrete equally spaced sets ω_x and ω_y of points be defined by

$$\omega_x = \{x(i) = ih_x, i = 0, 1, \dots, M; h_x M = l_x\}, \quad (1)$$

$$\omega_y = \{y(j) = jh_y, j = 0, 1, \dots, N; h_y N = l_y\}. \quad (2)$$

Computational grid Ω . Let a computational grid Ω on the domain G be a set of points defined by

$$\Omega = \omega_x \times \omega_y = \{\omega_{i,j} = (ih_x, jh_y), i = 0, 1, \dots, M, j = 0, 1, \dots, N\}.$$

Each (i, j) th node of the grid Ω refers to a point with $x(i)$ and $y(j)$ coordinates defined by Eqs. (1) and (2), respectively. The grid Ω is equally spaced in the x - and y -directions, but, in general, $h_x \neq h_y$.

Boundary and internal nodes. The nodes $(0, j)$, (M, j) , $(i, 0)$, (i, N) are boundary nodes. The nodes $[(i, j), i \neq 0 \text{ or } M, j \neq 0 \text{ or } N]$ are internal nodes.

Grid function $f_{i,j}$. Let a function $f(x, y)$ be defined on the domain G . A discrete function $f_{i,j} = f(x_i, y_j)$, where $x_i = x(i) \in \omega_x$, $y_j = y(j) \in \omega_y$ is a grid representation of $f(x, y)$ on the computational grid Ω .

Nine-point stencil $\sigma_{ij}^{(9)}$. Let (i, j) be an internal node in the computational grid Ω . Let a nine-point discretization stencil $\sigma_{ij}^{(9)}$ about a central node (i, j) be defined by

$$\sigma_{ij}^{(9)} = \{\omega_{p,q}, p = i - 1, i, i + 1, q = j - 1, j, j + 1\}, \quad (3)$$

where $\omega_{p,q} \in \Omega$.

Taylor series expansion on $\sigma_{ij}^{(9)}$. Let a discrete function $f_{i,j}$ be defined on $\sigma_{ij}^{(9)}$. A Taylor series expansion of $f_{i,j}$ about the central (i, j) node is

$$f_{i\pm 1, j\pm 1} = f_{i,j} + \sum_{m=1}^{\infty} \frac{1}{m!} (\pm h_x D_x \pm h_y D_y)^m f_{i,j}. \tag{4}$$

In Eq. (4), $D_x^m = \partial^m / \partial x^m$, $D_y^m = \partial^m / \partial y^m$ are differential operators.

Discrete equation on $\sigma_{ij}^{(9)}$. Let any linear relation between nine discrete values $u_{p,q}$ computed on $\sigma_{ij}^{(9)}$, i.e.,

$$\sum_{p=i-1}^{i+1} \sum_{q=j-1}^{j+1} \bar{a}_{pq} u_{p,q} = 0 \tag{5}$$

be a discrete equation for a function $u(x, y)$. Hereafter, the coefficients \bar{a}_{pq} will be termed the $\sigma_{ij}^{(9)}$ -stencil coefficients.

Modified equation on $\sigma_{ij}^{(9)}$. We consider a linear partial differential equation of the second-order in two independent variables

$$L^{(2)}u + L^{(1)}u + L^{(0)}u = f(x, y). \tag{6}$$

In Eq. (6), the operators $L^{(0)}$, $L^{(1)}$, and $L^{(2)}$ are

$$L^{(0)} = c, L^{(1)} = c_1 D_x + c_2 D_y, L^{(2)} = a_{11} D_x^2 + 2a_{12} D_x D_y + a_{22} D_y^2, \tag{7}$$

where $c, c_1, c_2, a_{11}, a_{12}, a_{22}$ are known coefficients, and $f(x, y)$ is a known function. Let us substitute Taylor series expansions (4) about the node $(i, j) \in \sigma_{ij}^{(9)}$ into the discrete Eq. (5) for each $u_{p,q}$. The Taylor series expansions (4), which include the differential operators, can formally be rearranged into the following form:

$$\hat{L}^{(2)}u_{i,j} + \hat{L}^{(1)}u_{i,j} + \hat{L}^{(0)}u_{i,j} = f_{i,j} + TE. \tag{8}$$

Here $\hat{L}^{(0)}$, $\hat{L}^{(1)}$, and $\hat{L}^{(2)}$ are operators

$$\hat{L}^{(0)} = \hat{c}, \hat{L}^{(1)} = \hat{c}_1 D_x + \hat{c}_2 D_y, \hat{L}^{(2)} = \hat{a}_{11} D_x^2 + 2\hat{a}_{12} D_x D_y + \hat{a}_{22} D_y^2, \tag{9}$$

where the coefficients $\hat{c}, \hat{c}_1, \hat{c}_2, \hat{a}_{11}, \hat{a}_{12}, \hat{a}_{22}$ depend on the coefficients \bar{a}_{pq} of the $\sigma_{ij}^{(9)}$ -stencil. The second term on the right-hand side of Eq. (8), which is called *the truncation error* (TE), consists of high-order derivatives, and can be expressed as

$$TE = \sum_{r=s \geq 3}^{\infty} \hat{L}^{(r)}u_{i,j}, \hat{L}^{(r)} = \sum_{m=0}^r \alpha_m h_x^m h_y^{r-m} D_x^m D_y^{r-m}. \tag{10}$$

If the $\sigma_{ij}^{(9)}$ -stencil coefficients, \bar{a}_{pq} , are chosen such that $\hat{L}^{(2)} = L^{(2)}$, $\hat{L}^{(1)} = L^{(1)}$, and $\hat{L}^{(0)} = L^{(0)}$, then Eq. (8) is called *the modified equation* [16] of Eq. (6). It is a finite-difference analog of the PDE, which is actually solved when the original Eq. (6) is discretized using a finite-difference approach. The TE is the difference between the original PDE and its approximated FDE. The lowest-order term of the TE gives the accuracy order of the discretization method applied to the original PDE. For example, the truncation error in Eq. (10) is of the $O(h^s)$ order.

We recall two commonly used methods for increasing the accuracy order of a finite-difference equation on a given discretization stencil: (a) the stencil coefficients \bar{a}_{pq} are chosen to provide

the accuracy order [s in Eq. (10)] as high as possible (in other words, as many as possible first terms of the TE are set to zero); (b) using the original PDE, as many as possible first terms in the TE are expressed in terms of the original PDE operators [$L^{(0)}$, $L^{(1)}$, and $L^{(2)}$ for Eq. (6)], and are moved to the left-hand side of the discrete equation; then the discretization stencil coefficients, \bar{a}_{pq} , are chosen in order that the discrete equation will be the modified one of the original PDE.

III. NINE-POINT $\sigma_{ij}^{(9)}$ -STENCIL FOR $\nabla^2 g = f(x, y)$

We consider the following Poisson equation for a function $g(x, y)$,

$$\nabla^2 g = f(x, y), \quad (11)$$

where $\nabla^2 = D_x^2 + D_y^2$ is the two-dimensional Laplacian operator ($D_x^2 = \partial^2 / \partial x^2$, $D_y^2 = \partial^2 / \partial y^2$). Our goal is to derive the discrete equation for Eq. (11) on the nine-point $\sigma_{ij}^{(9)}$ -stencil in the form

$$ag_{i,j} + bS_{i,j}^{g(xy)} + cS_{i,j}^{g(x)} + dS_{i,j}^{g(y)} = r_g, \quad (12a)$$

where

$$\begin{aligned} S_{i,j}^{g(xy)} &= g_{i-1,j-1} + g_{i-1,j+1} + g_{i+1,j-1} + g_{i+1,j+1}, \\ S_{i,j}^{g(x)} &= g_{i-1,j} + g_{i+1,j}, \quad S_{i,j}^{g(y)} = g_{i,j-1} + g_{i,j+1}. \end{aligned} \quad (12b)$$

In Ref. [13] the $\sigma_{ij}^{(9)}$ -stencil is developed for an elliptic equation of a special type: $\nabla^2 g - \gamma^2 g = -1$. Due to the symmetry of the sums $S_{i,j}^{g(xy)}$, $S_{i,j}^{g(x)}$, and $S_{i,j}^{g(y)}$ about the central (i, j) node, upon substituting the Taylor series expansions into Eq. (12), the resulting equation consists of only even-order derivatives: D_x^2 , D_y^2 , D_x^4 , $D_x^2 D_y^2$, D_y^4 , D_x^6 , $D_x^4 D_y^4$, \dots . The derivation of the $\sigma_{ij}^{(9)}$ -stencil coefficients is described in Appendix A. The coefficients are

$$\begin{aligned} a &= -2 \left(\frac{1}{h_x^2} + \frac{1}{h_y^2} \right) + 4b, \quad b = \frac{2}{4!} \left(\frac{1}{h_x^2} + \frac{1}{h_y^2} \right), \\ c &= \frac{1}{h_x^2} - 2b, \quad d = \frac{1}{h_y^2} - 2b \end{aligned} \quad (13a)$$

$$\begin{aligned} r_g &= f_{i,j} + \frac{1}{4!} (h_x^2 + h_y^2) (D_x^2 + D_y^2) f_{i,j} + \frac{2}{6!} (h_x^4 D_x^4 + 4h_x^2 h_y^2 D_x^2 D_y^2 + h_y^4 D_y^4) f_{i,j} \\ &\quad + \frac{1}{4!} (h_x^2 - h_y^2) (D_x^2 - D_y^2) f_{i,j} + \frac{3}{2 \cdot 6!} (h_x^2 - h_y^2)^2 D_x^2 D_y^2 f_{i,j}. \end{aligned} \quad (13b)$$

For $h_x = h_y = h$, the $\sigma_{ij}^{(9)}$ -stencil coefficients reduce to

$$\begin{aligned} a &= -\frac{10}{3h^2}, \quad b = \frac{1}{6h^2}, \quad c = d = \frac{2}{3h^2}, \\ r_g &= f_{i,j} + \frac{2h^2}{4!} \nabla^2 f_{i,j} + \frac{2h^4}{6!} (\nabla^4 f_{i,j} + 2D_x^2 D_y^2 f_{i,j}), \end{aligned}$$

as has already been shown in [1, 4, 8].

When the function $f(x, y)$ in Poisson equation is given analytically, the derivatives in the right-hand side terms of the equation in Eq. (13b) can be calculated exactly and present no difficulties. If $f(x, y)$ is given in a discrete form only at the grid nodes, then the differential operations in Eq. (13b) should be performed numerically and with the same accuracy as the discretization scheme itself. In any case, the right-hand side term in Eq. (13b) is computed (numerically or analytically) *ad hoc* before one starts solving the system of the discrete equations for the node values g_{ij} , and, therefore, does not bear additional computational effort. For the proposed discretization scheme, we use six terms of the Taylor series expansion and, hence, the truncation error of the scheme for $h_x \neq h_y$ is $O(h_x^4, h_x^2 h_y^2, h_y^4)$, while it is $O(h^6)$ for $h_x = h_y = h$.

IV. DISCRETIZATION OF A BIHARMONIC EQUATION

We consider a biharmonic equation for a function $u(x, y)$,

$$\nabla^4 u \equiv (D_x^2 + D_y^2)^2 u = (D_x^4 + 2D_x^2 D_y^2 + D_y^4) u = f(x, y). \quad (14)$$

This equation can be split into two coupled equations:

$$\nabla^2 v = f(x, y) \quad (15a)$$

$$\nabla^2 u = v(x, y). \quad (15b)$$

We write the discrete equations for Eqs. (15a) and (15b) on a nine-point $\sigma_{ij}^{(9)}$ -stencil in the form

$$av_{i,j} + bS_{i,j}^{v(xy)} + cS_{i,j}^{v(x)} + dS_{i,j}^{v(y)} = r_v, \quad (16a)$$

$$au_{i,j} + bS_{i,j}^{u(xy)} + cS_{i,j}^{u(x)} + dS_{i,j}^{u(y)} = r_u. \quad (16b)$$

Equations (15) are Poisson equations and their discrete form, Eqs. (16), on a $\sigma_{ij}^{(9)}$ -stencil have been derived in the previous section. The coefficients a, b, c, d are defined by Eqs. (13a). The right-hand side term r_v is defined by Eq. (13b), while for r_u from Eq. (13b) we have

$$\begin{aligned} r_u = v_{i,j} + \frac{1}{4!}(h_x^2 + h_y^2)f_{i,j} + \frac{2}{6!}(h_x^4 D_x^4 + 4h_x^2 h_y^2 D_x^2 D_y^2 + h_y^4 D_y^4)v_{i,j} \\ + \frac{1}{4!}(h_x^2 - h_y^2)(D_x^2 - D_y^2)v_{i,j} + \frac{3}{2 \cdot 6!}(h_x^2 - h_y^2)^2 D_x^2 D_y^2 v_{i,j}, \end{aligned} \quad (17)$$

where for the second term of Eq. (13b) we have used $(D_x^2 + D_y^2)v_{i,j} = f_{i,j}$. The derivatives in Eq. (17) should be calculated numerically. Here we suggest an effective procedure, using the $\sigma_{ij}^{(9)}$ -stencil, to compute them with the same high-order accuracy as the discretization scheme. First, it is readily seen from the discretization stencil definition, Eq. (12b), that

$$\begin{aligned} D_x^2 D_y^2 v_{i,j} &= \frac{1}{h_x^2 h_y^2} (S_{i,j}^{v(xy)} - 2S_{i,j}^{v(x)} - 2S_{i,j}^{v(y)} + 4v_{i,j}) + O(h_x^2, h_y^2) \\ D_x^2 v_{i,j} &= \frac{1}{h_x^2} (S_{i,j}^{v(x)} - 2v_{i,j}) - \frac{h_x^2}{12} D_x^4 v_{i,j} + O(h_x^4) \\ D_y^2 v_{i,j} &= \frac{1}{h_y^2} (S_{i,j}^{v(y)} - 2v_{i,j}) - \frac{h_y^2}{12} D_y^4 v_{i,j} + O(h_y^4). \end{aligned} \quad (18)$$

Second, from Eq. (15a) we have

$$D_x^4 v_{i,j} = D_x^2 f_{i,j} - D_x^2 D_y^2 v_{i,j}$$

$$D_y^4 v_{i,j} = D_y^2 f_{i,j} - D_x^2 D_y^2 v_{i,j}. \tag{19}$$

Thus, one can see that computing the derivatives in Eq. (17) with the aid of the expressions in Eqs. (18) and (19) gives the sixth-order accuracy for r_u : $O(h_x^6, h_x^4 h_y^2, h_x^2 h_y^4, h_y^6)$.

The high-order accuracy discretization scheme for a biharmonic equation as developed in this section is appropriate to internal nodes of the computational domain. The original biharmonic equation is split into two Poisson equations. If the Dirichlet boundary conditions can be imposed for both equations, then the only source of errors in the numerical solution arises from the discretization of the governing equation. If the boundary conditions involve calculation of derivatives at the boundary, they should be written in a discrete form with at least the same truncation error as the discretization scheme used for the governing equation. The lower accuracy of the solution at the boundary will contaminate the accuracy of the numerical solution in the interior nodes. The high-order accuracy discretization of the mixed boundary conditions for Eq. (14) is developed in Appendix B.

V. NUMERICAL RESULTS

The biharmonic equation in Eq. (14) describes the deflections of loaded plates and is used in the theory of plates. The analytical and approximate methods for solving this equation are widely discussed in the literature [1, 17]. In this section we consider the deflections of a rectangular plate for two different cases of boundary conditions: (1) a simply supported plate and (2) a plate with built-in edges. Both cases are well known in the classical literature on the theory of plates and we choose them to test the high-accuracy discretization scheme developed in the course of this study. We present numerical results for the high-order accuracy scheme developed here and compare them with exact solutions as well as with the results obtained using a standard second-order accuracy finite-difference scheme. In cases when the exact (analytical) solution is unknown, we apply a commonly used technique suggested by Richardson [18] for estimating the final truncation-converted solution for $O(h^k)$ numerical schemes. According to the Richardson extrapolation, we write a Taylor series for the exact solution $u^{(e)}$,

$$u^{(e)} = u^{(h)} + bh^k + O(h^k), \quad u^{(e)} = u^{(2h)} + b(2h)^k + O(h^k), \tag{20}$$

where $u^{(h)}$ and $u^{(2h)}$ are numerical solutions obtained with two successive grids. For a small grid spacing h , by eliminating b from these equations, the truncation-converted (exact) solution can be estimated as

$$u^{(e)} = \frac{2^k}{2^k - 1} u^{(h)} - \frac{1}{2^k - 1} u^{(2h)}. \tag{21}$$

For the sixth-order accuracy scheme developed here $k = 6$, and for the standard finite-difference scheme, $k = 2$.

A. Case 1: A Simply Supported Plate

Consider a rectangular plate $\{0 \leq x \leq a, 0 \leq y \leq b\}$, which is freely mounted along the edges. This is the case of a simply supported plate. The boundary conditions are [17]

$$\begin{aligned} u = 0, \quad \frac{\partial^2 u}{\partial x^2} = 0 \quad \text{for } x = 0 \text{ and } x = a \\ u = 0, \quad \frac{\partial^2 u}{\partial y^2} = 0 \quad \text{for } y = 0 \text{ and } y = b. \end{aligned} \quad (22)$$

This case is relatively simple, because the system of Eqs. (15) can be decoupled into two Poisson equations with Dirichlet boundary conditions for both functions:

$$\nabla^2 v = f(x, y), \quad v|_{\Gamma} = 0 \quad (23a)$$

and

$$\nabla^2 u = v(x, y), \quad u|_{\Gamma} = 0. \quad (23b)$$

We consider two cases of load distribution over the plate surface:

$$\text{Case 1a: } f(x, y) = \pi^4 \left(\frac{m^2}{a^2} + \frac{n^2}{b^2} \right)^2 \sin \frac{m\pi x}{a} \sin \frac{n\pi y}{b}. \quad (24a)$$

$$\text{Case 1b: } f(x, y) = \frac{q}{\pi} \sum_{i=1}^2 \sum_{j=1}^2 e^{-\frac{(x-x_i)^2 + (y-y_j)^2}{\alpha_{ij}}}. \quad (24b)$$

Case 1a (sinusoidal load) can be solved analytically and the exact solution is

$$u(x, y) = \sin \frac{m\pi x}{a} \sin \frac{n\pi y}{b}. \quad (25)$$

Case 1b, for small values of α_{ij} , is a plate under loads that are concentrated at four points $(x_i, y_j, i, j = 1, 2)$. This case can be solved only numerically. In our calculations we specify: $q = 10^4$, $\alpha_{ij} = 0.01$, $x_1 = 0.2$, $x_2 = 0.8$, $y_1 = 0.2$, $y_2 = 0.8$.

The numerical solution error (Case 1a) is plotted in Fig. 1 for different grid spacings. Here $\text{Error} = \|u_{ij} - u_{ij}^{(e)}\|_{rms}$, where the exact solution $u_{ij}^{(e)}$ is evaluated from Eq. (25) at each (i, j) th node. The slope of the line is the accuracy order. Figure 1(a) (equally spaced grid) clearly illustrates the sixth-order accuracy (the slope is 6) of the suggested high-order discretization, while for the standard finite-difference scheme the accuracy is of the second-order (the slope is 2). The case with $m = n = 3$ is more difficult to compute due to the oscillating behavior of the solution. In this case the global error is higher, while the numerical solution accuracies (line slopes) are of the same order as for $m = n = 1$. The numerical solution error for the unequally spaced ($h_x = 2h_y$) grid is shown in Fig. 1(b). For $m = 1$, $n = 3$, the results, as expected, show the fourth- and second-order numerical errors for the suggested high-order accuracy and standard finite-difference schemes, respectively. For $m = n = 3$, the accuracy of the high-order scheme is of the sixth-order (the slope is 6), despite the unequally spaced grid that is used. This happened accidentally, because the leading term in the truncation error in Eq. (A10) (Appendix A) is equal to zero due to $x \leftrightarrow y$ symmetry of the solution.

As mentioned earlier, the example in Case 1b cannot be solved analytically. The plots of the loading function, $f(x, y)$, and the numerical solution, $u(x, y)$, as obtained with the high-order

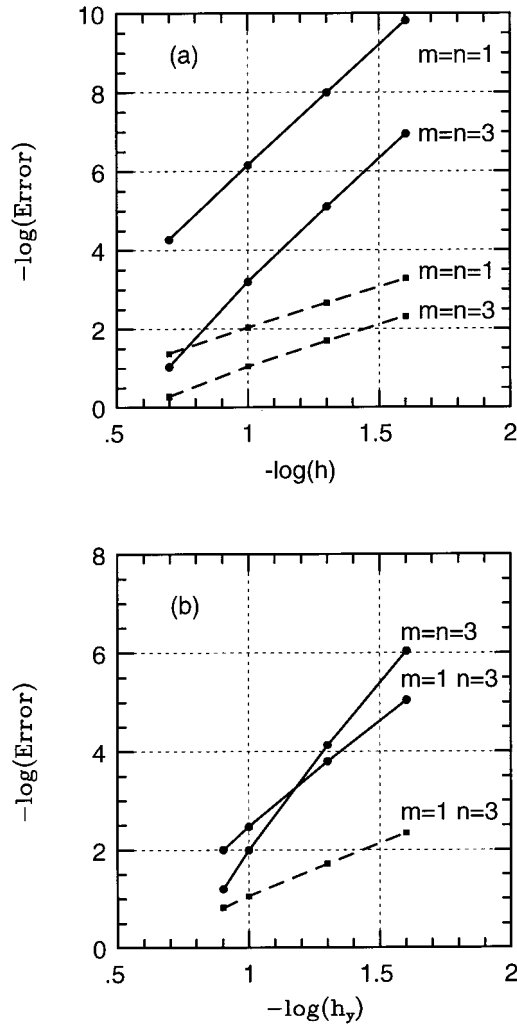


FIG. 1. Case 1a. Numerical solution error for different computational grids; solid line—high-order, dashed line—standard finite-difference, a—equally spaced grid, b—unequally spaced grid.

accuracy discretization scheme are shown in Fig. 2. In such cases usually the convergence of the numerical results with grid refinement is analyzed when the “exact” (truncation-converted) solution is estimated using the Richardson extrapolation from Eq. (21). The numerical solution error (Case 1b), $\text{Error} = \|u_{ij} - u_{ij}^{(e)}\|_{rms}$, where the exact solution $u_{ij}^{(e)}$ is estimated at each (i, j) th node is presented in Fig. 3(a). The slope of the line is the accuracy order. Figure 3(a) shows the sixth-order accuracy (the slope is 6) of the suggested high-order discretization for the fine grid, while for the standard finite-difference scheme the accuracy is of the second-order (the slope is 2). The values of $u(x, y)$ at two points computed with three successive computation meshes are presented in Fig. 3(b). The close-to-constant behavior of the high-order accuracy scheme results (solid lines) boldly illustrates the convergence even on a coarse grid. On the other hand, it is seen that the results obtained on the three successive meshes with the standard second-order accuracy

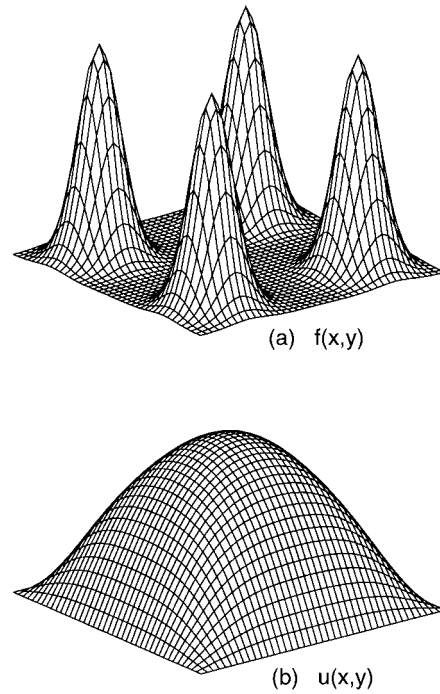


FIG. 2. Case 1b. Surfaces of (a) the loading function and (b) the high-order accuracy numerical solution.

finite-difference scheme (dashed lines) are different, and only the results on the finest grid could be considered as converged.

B. Case 2: A Plate with Built-In Edges

If a thin rectangular plate is clamped along one of its sides (the edge is built-in), the deflection along this side is zero. The tangent plane to the deflected middle surface along this edge coincides with the initial position of the middle plane of the plate. The boundary conditions for a rectangular plate with all edges built-in are [17]

$$u = 0, \frac{\partial u}{\partial x} = 0 \text{ for } x = 0 \text{ and } x = a$$

$$u = 0, \frac{\partial u}{\partial y} = 0 \text{ for } y = 0 \text{ and } y = b. \quad (26)$$

Numerical and approximated methods for solving the problem of deflections of the clamped plate were a subject of intensive investigations from the turn of this century. Due to the mixed boundary conditions the system of equations in Eqs. (15) cannot be decoupled. It means that though the problem for $u(x, y)$, Eq. (26), is defined with the Dirichlet condition ($u|_{\Gamma} = 0$), the boundary conditions for $v(x, y)$ cannot be specified independently. The Neumann-type boundary condition ($\partial u / \partial n = 0$) should be discretized with the same high-order accuracy as the discretization scheme, and we used the method suggested in Appendix B.

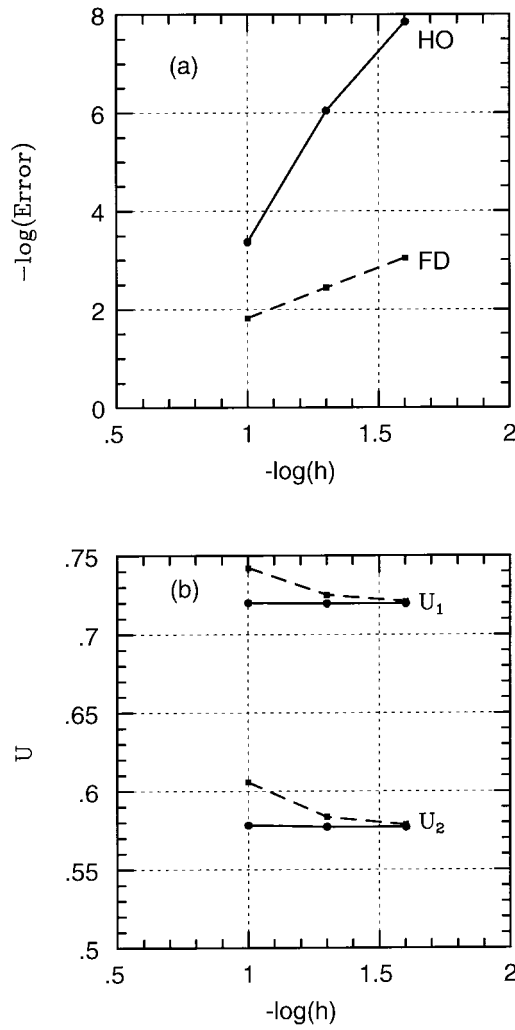


FIG. 3. Case 1b. (a) Numerical solution error and (b) solution at two points for different computational grids; solid line—high-order, dashed line—standard finite-difference.

We consider two cases of load distribution over the surface of the clamped plate:

$$\text{Case 2a: } f(x, y) = 56400(a^2 - 10ax + 15x^2)(b - y)^2y^4 + 18800x^2(6a^2 - 20ax + 15x^2) \times y^2(6b^2 - 20by + 15y^2) + 56400(a - x)^2x^4(b^2 - 10by + 15y^2). \quad (27a)$$

$$\text{Case 2b: } f(x, y) = p_0 = \text{Const.} \quad (27b)$$

Case 2a can be solved analytically, and the exact solution is

$$u(x, y) = 2350x^4(x - a)^2y^4(y - b)^2. \quad (28)$$

Case 2b (uniform load) is very important in the theory of plates and cannot be solved analytically. Thus, the case of a uniformly loaded plate is a subject of numerical analysis and the first numerical

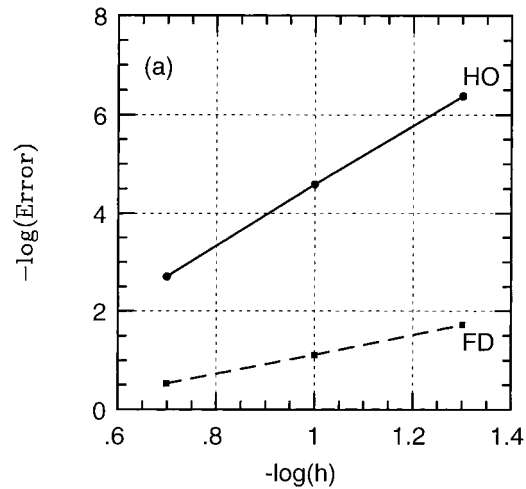


FIG. 4. Case 2a. Numerical solution error for different computational grids; equally spaced grid, solid line—high-order, dashed line—standard finite-difference.

results are referred in [17] to 1902. An approximate solution based on Fourier-series expansion is discussed in detail in [1, 17]. This solution is fairly cumbersome and its implementation is complicated.

The numerical solution error (Case 2a), $Error = \|u_{ij} - u_{ij}^{(e)}\|_{rms}$, where the exact solution $u_{ij}^{(e)}$ is estimated from Eq. (28) at each (i, j) th node is plotted in Fig. 4. The slope of the line is the accuracy order. Figure 4 illustrates the sixth-order accuracy (the slope is 6) of the suggested high-order discretization, while for the standard finite-difference scheme the accuracy is of the second-order (the slope is 2).

As mentioned earlier, the example in Case 2b (uniform load) cannot be solved analytically and we estimate the truncation-converted (exact) solution using the Richardson extrapolation from Eq. (21). The numerical solution error (Case 2b, $p_0 = 10^3$), $Error = \|u_{ij} - u_{ij}^{(e)}\|_{rms}$ is presented in Fig. 5(a). The slope of the line in Fig. 5(a) shows the sixth-order accuracy (the slope is 6) of the suggested high-order discretization for the fine grid, while for the standard finite-difference scheme the accuracy is of the second-order (the slope is 2). In Fig. 5(b) the values of $u(x, y)$ at two points computed with three successive computation meshes are presented. The close-to-constant behavior of the high-order accuracy scheme results (solid lines) boldly illustrates the convergence even on a coarse grid. On the other hand, it is seen that the results obtained on the three successive meshes with the standard second-order accuracy finite-difference scheme (dashed lines) are different, and only the results on the finest grid could be considered as converged.

VI. CONCLUSIONS

The coefficients for a nine-point high-order accuracy discretization scheme for a biharmonic equation $\nabla^4 u = f(x, y)$ (∇^2 is the two-dimensional Laplacian operator) are derived. The biharmonic problem is defined on a rectangular domain with two types of boundary conditions: (1) u and $\partial^2 u / \partial n^2$ or (2) u and $\partial u / \partial n$ (where $\partial / \partial n$ is the normal to the boundary derivative) are

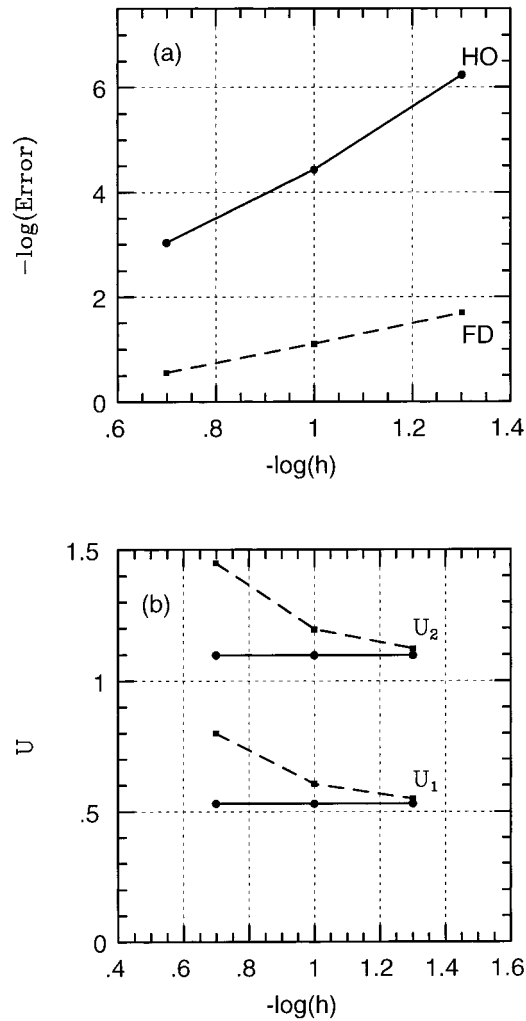


FIG. 5. Case 2b. (a) Numerical solution error and (b) solution at two points for different computational grids; solid line—high-order, dashed line—standard finite-difference.

specified at the boundary. For both cases, the truncation error for the scheme is of the sixth-order $O(h^6)$ on a square mesh ($h_x = h_y = h$) and of the fourth-order $O(h_x^4, h_x^2 h_y^2, h_y^4)$ on an unequally spaced mesh. The advantage of the suggested scheme is demonstrated for solving problems of the deflections of a rectangular plate for different cases of boundary conditions: (1) a simply supported plate and (2) a plate with built-in edges. The numerical results obtained with the developed high-order accuracy discretization scheme are compared with exact solutions and with the results of calculations based on the standard second-order accuracy finite-difference scheme.

APPENDIX A: DERIVATION OF THE $\sigma_{ij}^{(9)}$ -STENCIL COEFFICIENTS

Let

$$au_{i,j} + bS_{i,j}^{(xy)} + cS_{i,j}^{(x)} + dS_{i,j}^{(y)} = r_0 \tag{A1}$$

be a discrete equation on the nine-point $\sigma_{ij}^{(9)}$ -stencil, where

$$S_{i,j}^{(xy)} = u_{i-1,j-1} + u_{i-1,j+1} + u_{i+1,j-1} + u_{i+1,j+1},$$

$$S_{i,j}^{(x)} = u_{i-1,j} + u_{i+1,j}, S_{i,j}^{(y)} = u_{i,j-1} + u_{i,j+1}. \tag{A2}$$

The Taylor series expansions on $\sigma_{ij}^{(9)}$ are

$$u_{i\pm 1,j\pm 1} = u_{i,j} + \sum_{m=1}^{\infty} \frac{1}{m!} (\pm h_x D_x \pm h_y D_y)^m u_{i,j}. \tag{A3}$$

Substituting expansions (A3) into (A2) leads to

$$S_{i,j}^{(xy)} = 4u_{i,j} + 4 \sum_{m=1}^{\infty} \sum_{n=0}^m \frac{h_x^{2m-2n} h_y^{2n}}{(2m-2n)!(2n)!} D_x^{2m-2n} D_y^{2n} u_{i,j}$$

$$S_{i,j}^{(x)} = 2u_{i,j} + 2 \sum_{m=1}^{\infty} \frac{h_x^{2m}}{(2m)!} D_x^{2m} u_{i,j}, S_{i,j}^{(y)} = 2u_{i,j} + 2 \sum_{m=1}^{\infty} \frac{h_y^{2m}}{(2m)!} D_y^{2m} u_{i,j}. \tag{A4}$$

High-order accuracy schemes result from higher order Taylor polynomials. Substituting Eq. (A4) into Eq. (A1) and keeping derivatives up to the sixth order in the left-hand side give

$$\left[(4b + 2c) \left(\frac{h_x^2}{2!} D_x^2 + \frac{h_x^4}{4!} D_x^4 + \frac{h_x^6}{6!} D_x^6 \right) + (4b + 2d) \left(\frac{h_y^2}{2!} D_y^2 + \frac{h_y^4}{4!} D_y^4 + \frac{h_y^6}{6!} D_y^6 \right) \right. \\ \left. + 4b \left(\frac{h_x^2 h_y^2}{2!2!} D_x^2 D_y^2 + \frac{h_x^4 h_y^2}{4!2!} D_x^4 D_y^2 + \frac{h_x^2 h_y^4}{2!4!} D_x^2 D_y^4 \right) + (a + 4b + 2c + 2d) \right] u_{i,j}$$

$$= r_0 + TE. \tag{A5}$$

Using Eq. (11) enables one to rewrite the high-order derivative operators in the left-hand side of Eq. (A5) as

$$D_x^4 u = D_x^2 f - D_x^2 D_y^2 u, D_y^4 u = D_y^2 f - D_x^2 D_y^2 u,$$

$$D_x^6 u = D_x^4 f - D_x^4 D_y^2 u, D_y^6 u = D_y^4 f - D_x^2 D_y^4 u. \tag{A6}$$

Substituting Eqs. (A6) into Eq. (A5) gives

$$(\hat{a}_{11} D_x^2 + 2\hat{b} D_x^2 D_y^2 + \hat{a}_{22} D_y^2 + \hat{a}_{00}) u_{i,j} + (g_{42} D_x^4 D_y^2 + g_{24} D_x^2 D_y^4) u_{i,j} = r_0 + TE, \tag{A7}$$

where $g_{42} = g(h_x, h_y; b, c, d)$, $g_{24} = g(h_y, h_x; b, d, c)$. We note that for equally spaced grid $h_x = h_y = h$, due to $x \leftrightarrow y$ symmetry of the elliptic equation, $c = d$ in Eq. (A1), and, hence, $g_{42} = g_{24}$. Therefore, it is useful to rewrite the second term on the left-hand side of Eq. (A7) as a sum of symmetric and asymmetric terms

$$g_{42} D_x^4 D_y^2 + g_{24} D_x^2 D_y^4 \equiv \frac{g_{42} + g_{24}}{2} (D_x^4 D_y^2 + D_x^2 D_y^4) + \frac{g_{42} - g_{24}}{2} (D_x^4 D_y^2 - D_x^2 D_y^4), \tag{A8}$$

because the second (asymmetric) term in Eq. (A8) vanishes on the equally spaced grid. The first (symmetric) term in Eq. (A8) could be rewritten as

$$\frac{g_{42} + g_{24}}{2} (D_x^4 D_y^2 + D_x^2 D_y^4) u_{i,j} = \frac{g_{42} + g_{24}}{2} D_x^2 D_y^2 f_{i,j}. \tag{A9}$$

Finally, replacing the first right-hand side term of Eq. (A8) by Eq. (A9), adding it to the mixed derivative term of Eq. (A7), and moving the second term of Eq. (8) (which is actually the leading term of the truncation error) to the right-hand side of Eq. (A7), complete the rearrangement of the discrete equation, which now reads

$$(\hat{a}_{11}D_x^2 + 2\hat{a}_{12}D_x^2D_y^2 + \hat{a}_{22}D_y^2 + \hat{a}_{00})u_{i,j} = r_0 + TE. \quad (\text{A10})$$

Here the truncation error is estimated as

$$TE \approx \frac{g_{42} - g_{24}}{2}(D_x^4D_y^2 - D_x^2D_y^4)u_{i,j} + O(h_x^6, h_x^4h_y^2, h_x^2h_y^4, h_y^6). \quad (\text{A11})$$

We note that for an unequally spaced grid g_{42} and g_{24} are of the fourth-order $O(h_x^4, h_x^2h_y^2, h_y^4)$. For an equally spaced grid, $g_{42} = g_{24}$ and the discretization scheme becomes of the sixth-order accuracy $O(h^6)$.

The coefficients \hat{a}_{pq} in Eq. (A10) depend on the grid spacings (h_x and h_y) and on the $\sigma_{ij}^{(9)}$ -stencil coefficients a, b, c, d . In order for Eq. (A10) to become the modified equation of the original Poisson equation, Eq. (11), we require

$$\hat{a}_{00} = 0, \hat{a}_{11} = 1, \hat{a}_{12} = 0, \hat{a}_{22} = 1, \quad (\text{A11})$$

which is a linear system for four unknown coefficients a, b, c, d . We omit simple algebra and summarize the coefficients in Eqs. (13).

APPENDIX B: MIXED BOUNDARY CONDITIONS

We consider the $y = 0$ boundary, where the mixed boundary conditions are imposed

$$u|_{y=0} = p(x), Du|_{y=0} \equiv D_{y0}u = g(x). \quad (\text{B1})$$

The same discretization procedure of the mixed boundary conditions can be applied at each boundary of the given rectangular. For simplicity we provide the discretization for the $y = 0$ boundary. Here and hereafter, the subscript 0 denotes that the function or its derivative is calculated at $y = 0$. The subscripts 1, 2, and 3 stand for the values at the first, second, and third nodes, respectively. Let us write the Taylor series for the node values $u_1, u_2, u_3, v_1, v_2, v_3$:

$$u_1 = u_0 + \sum_{m=1}^7 \frac{h_y^m}{m!} D_{y0}^m u, \quad u_2 = u_0 + \sum_{m=1}^7 \frac{(2h_y)^m}{m!} D_{y0}^m u, \quad u_3 = u_0 + \sum_{m=1}^7 \frac{(3h_y)^m}{m!} D_{y0}^m u,$$

$$v_1 = v_0 + \sum_{m=1}^5 \frac{h_y^m}{m!} D_{y0}^m v, \quad v_2 = v_0 + \sum_{m=1}^5 \frac{(2h_y)^m}{m!} D_{y0}^m v, \quad v_3 = v_0 + \sum_{m=1}^5 \frac{(3h_y)^m}{m!} D_{y0}^m v. \quad (\text{B2})$$

Using the original equations in Eqs. (15) and simple calculus, the u -derivatives at the boundary $y = 0$ can be expressed in terms of the v -derivatives and given boundary conditions in Eq. (B1), viz.

$$D_{y0}^2 u = v_0 - D_x^2 p, \quad D_{y0}^3 u = D_{y0} v - D_x^2 g,$$

$$D_{y0}^4 u = 2D_{y0}^2 v + D_x^4 p - f, \quad D_{y0}^5 u = 2D_{y0}^3 v + D_x^4 g - D_{y0} f$$

$$D_{y_0}^6 u = 3D_{y_0}^4 v - D_x^6 p - 2D_{y_0}^2 f + D_x^2 f$$

$$D_{y_0}^7 u = 3D_{y_0}^5 v - D_x^6 g - 2D_{y_0}^3 f + D_x^2 D_{y_0} f. \quad (\text{B3})$$

Finally, substituting the expressions in Eqs. (B3) into Eqs. (B2) and eliminating the derivatives $D_{y_0}^k v$ ($k = 1, 2, \dots, 5$) lead to the following relation for the node values:

$$\frac{5}{h_y^2} (16848u_1 - 567u_2 - 16u_3) + 6(-3962v_0 - 2484v_1 + 459v_2 - 28v_3)$$

$$= -18(75h_y^2 - 12h_y^3 D_{y_0} - 24h_y^4 D_{y_0}^2 + 12h_y^4 D_x^2$$

$$- 10h_y^5 D_{y_0}^3 + 5h_y^5 D_x^2 D_{y_0})f - 18(2005D_x^2 - 75h_y^2 D_x^4 - 12h_y^4 D_x^6)p$$

$$- 18(550h_y D_x^2 + 12h_y^3 D_x^4 - 5h_y^5 D_x^6)g + \frac{81325p}{h_y^2} + \frac{78330g}{h_y}. \quad (\text{B4})$$

This equation should be added to the global system of the discretization scheme. It is seen from Eqs. (B2) that the discrete analog [Eq. (B4)] of the boundary conditions [Eqs. (B1)] is derived with the sixth-order accuracy.

References

1. L. V. Kantorovich and V. I. Krylov, *Approximation Methods of Higher Analysis*, Interscience, New York, 1964.
2. L. Collatz, *The Numerical Treatment of Differential Equations*, Springer-Verlag, Berlin, 1960.
3. D. M. Young and J. H. Dawwalder, "Discrete representations of partial differential equations," in *Errors in Digital Computation*, L. B. Rall, Ed., Wiley, New York, 1965.
4. D. M. Young and R. T. Gregory, *A Survey of Numerical Mathematics*, Vol II, Addison-Wesley, Reading, MA, 1973.
5. R. E. Lynch and J. R. Rice, "The HODIE method and its performance for solving elliptic partial differential equations," in *Recent Developments in Numerical Analysis*, C. de Boor, Ed., Academic, New York, 1978, pp. 143-175.
6. R. F. Boisvert, "Families of high order accurate discretizations of some elliptic problems." *SIAM J. Sci. Stat. Comput.* **2**, 268-284, 1981.
7. E. N. Houstis and T. S. Papatheodorou, "A sixth order fast Helmholtz equation solver and its performance," *Advances in Computer Methods for Partial Differential Equations*, Vol. III, R. Vichnevetsky, Ed., IMACS, New Brunswick, NJ, 1979, pp. 13-18.
8. R. Manohar and J. W. Stephenson, "New high order difference methods for solving the Poisson equation," *Congressus Numerantium* **34**, 483-493 (1982).
9. R. Manohar and J. W. Stephenson, "Single cell high order methods for Helmholtz equation," *J. Comput. Phys.* **51**, 444-453 (1983).
10. R. Manohar and J. W. Stephenson, "High order difference scheme for linear partial differential equations," *SIAM J. Sci. Stat. Comput.* **5**, 69-77 (1984).
11. M. M. Gupta, R. Manohar, and J. W. Stephenson, "High-order difference scheme for two-dimensional elliptic equations," *Numer. Meth. Partial Differential Eq.* **1**, 71-80 (1985).
12. U. Anathakrishnaiah, R. Manohar, and J. W. Stephenson, "High-order methods for elliptic equations with variable coefficients," *Numer. Meth. Partial Differential Eq.* **3**, 219-227 (1987).
13. M. Arad, A. Yakhot, and G. Ben-Dor, "High-order-accurate discretization stencil for an elliptic equation," *Int. J. Num. Methods in Fluids*, **23**, 367-377 (1996).

14. Y. Kwon, R. Manohar, and J. W. Stephenson, "Single cell fourth order methods for the biharmonic equation," *Congressus Numerantium* **34**, 475–482 (1982).
15. J. W. Stephenson, "Single cell discretizations of order two and four for biharmonic problems," *J. Comput. Phys.* **55**, 65–80 (1984).
16. D. A. Anderson, J. C. Tannehill, and R. H. Pletcher, *Computational Fluid Mechanics and Heat Transfer*, Hemisphere, Washington (1984).
17. S. P. Timoshenko and S. Woinowsky-Krieger, *Theory of Plates and Shells*, McGraw-Hill, New York (1970).
18. L. F. Richardson, "The approximate arithmetical solution by finite difference of physical problems involving differential equations with an application to the stress in Masonry dam," *Transaction of the Royal Society of London, Ser. A.*, **210**, 307–357 (1910).